Karim, Altaf; Al-Rawi, Ahlam N.; Kara, Abdelkader; Rahman, Talat S.; Trushin, Oleg; Ala-Nissilä, Tapio

Diffusion of small two-dimensional Cu islands on Cu(111) studied with a kinetic Monte Carlo method

Diffusion of small two-dimensional Cu islands on Cu(111) studied with a kinetic Monte Carlo method

Altaf Karim, Ahlam N. Al-Rawi, Abdelkader Kara, and Talat S. Rahman
Department of Physics, Cardwell Hall, Kansas State University, Manhattan, Kansas 66506, USA

Oleg Trushin
Institute of Microelectronics and Informatics, Academy of Sciences of Russia, Yaroslavl 150007, Russia

Tapio Ala-Nissila
*Laboratory of Physics, P.O. Box 1100, Helsinki University of Technology, FIN-02015 TKK, Espoo, Finland
and Department of Physics, Brown University, Providence, Rhode Island 02912-1843, USA*

Diffusion of small two-dimensional Cu islands (containing up to 10 atoms) on Cu(111) has been studied using the newly developed self-learning Kinetic Monte Carlo (SLKMC) method which is based on a database of diffusion processes and their energetics accumulated automatically during the implementation of the SLKMC code. Results obtained from simulations in which atoms hop from one fcc hollow site to another are compared with those obtained from a parallel set of simulations in which the database is supplemented by processes revealed in complementary molecular dynamics simulations at 500 K. They include processes involving the hcp (stacking-fault) sites, which facilitate concerted motion of the islands (simultaneous motion of all atoms in the island). A significant difference in the scaling of the effective diffusion barriers with island size is observed in the two cases. In particular, the presence of concerted island motion leads to an almost linear increase in the effective diffusion barrier with size, while its absence accounts for strong size-dependent oscillations and anomalous behavior for trimers and heptamers. We also identify and discuss in detail the key microscopic processes responsible for the diffusion and examine the frequencies of their occurrence, as a function of island size and substrate temperature.

I. INTRODUCTION

Acquiring a precise knowledge of the microscopic mechanisms responsible for island diffusion or mass transport on surfaces is an important step towards the understanding of phenomena such as thin film growth and its morphological evolution. Motivated by experimental observations, initially using field ion microscopy (FIM),[1–6] and more recently with the use of the scanning tunneling microscope (STM),[7–15] the study of adatom and vacancy island diffusion as a function of size has been an important concern also for many theorists[16–25] Because of the inherent differences in the microscopic processes responsible for the diffusion and its scaling behavior with size, the discussion has naturally bifurcated into those for the larger islands, usually containing more than 20 atoms, and the smaller ones ($N < 20$). For the larger islands, the diffusion coefficients appear to scale as a function of the size and the scaling exponent is expected to reflect the intervening atomistic processes responsible for the diffusion.[20,26] However, for the smaller islands a consistent knowledge of the variation of their mobility with size and the details of the responsible atomistic processes has not yet been fully established, especially on the (111) surfaces of fcc metals.

One of the distinguishing geometrical features of the fcc(111) surface is the presence of two types of hollow sites: the so-called fcc site under which there is no atom in the second layer and whose occupancy by an adatom maintains the crystal stacking order, and the hcp site under which there is an atom in the second layer and its nucleation can lead to a stacking fault. Whether or not an adatom or atoms in an adatom island occupy one or the other of these two sites depends on their relative occupation energies and has significant consequences for epitaxial growth and the morphological evolution of the surface. Although Ag, Cu, Pt, and Ir are all fcc crystals there is no guarantee that the adatom would prefer to sit in the fcc site. In fact, experiments show that the hcp site is preferred on Ir(111),[3,15] while on Cu(111) the fcc site appears to be favored,[9] although the small difference in the occupation energy (a few meV) between the two sites does not rule out the occupation of the hcp sites. For dimers, trimers, and other larger islands, mixed occupancy of the two sites is also possible. The relative probability of occupancy of these two sites on fcc(111) surfaces continues to be the subject of much discussion and debate.

For small adatom islands earlier experimental studies point to a general decrease in mobility with increasing island size, except for some cases of anomalously large mobility.[1–6] For larger islands short-range diffusion of the atoms around the periphery, followed by adjustment of island shape, has been proposed to be the dominant mechanism for the diffusion.[3,17] In the case of small Ir islands on Ir(111), concerted gliding motion of the island has also been reported.[3] Subsequent molecular dynamics (MD) simulations using

many-body potentials based on the embedded atom method (EAM) (Ref 27) have further disclosed that in addition to gliding, there is simultaneous motion of a portion of the island from the fcc to the hcp sites, creating a stacking fault.[18] The motion of the island could result from the rest of the atoms shifting also to the available hcp site. On Ni(111), for example, the smaller islands reportedly find the fcc to hcp transition to be critical to their diffusion, although gliding of the island as a whole and periphery motion has also been seen.[18] In agreement with the experimental results of Wang and Ehrlich on the higher mobility of tetramers as compared to trimers for Ir on Ir(111), Chang *et al.*[21] find the barrier for diffusion for the tetramer to be lower than that for the trimer for a number of fcc metals. They also predict a zig-zag motion to be the dominant one for the dimer and the tetramer, while predicting a concerted motion as a whole for the trimer. Recent theoretical studies of the energetics and dynamics of 1–7 atom Cu islands on Cu(111) have once again highlighted the role of the concerted motion of the island in controlling its diffusion characteristics.[28] In the very recent work of Mueller *et al.*[16] good agreement with experimental data on submonolayer epitaxy on Ir(111) is also obtained with the inclusion of concerted motion of islands (with the stacking fault sites). Issues about the relative importance of the proposed diffusion mechanisms, the relevance of the occupation of the hcp sites, and the observed anomalous diffusion for certain sizes, are striking aspects of the diffusion of small 2D islands on fcc(111) surfaces and may control the subsequent growth patterns on these surfaces.

Our purpose here is to determine the microscopic factors that control the diffusion of small Cu islands on Cu(111) in an unbiased manner. We should hasten to mention that some results for such systems have recently been presented by Marinica *et al.*[28] who focused on the application of a newer version of the EAM potentials[29] to calculate diffusion barriers and pre-exponential factors for a small set of likely processes that they find from MD simulations to be responsible for island diffusion. The work ignores the contribution of mechanisms associated with atom-by-atom motion in small islands and attributes the diffusion to specific collective island motion. The diffusion coefficient is simply obtained from application of the Arrhenius law to the activation energy barrier and the diffusion prefactor calculated for the chosen diffusion process. The natural question is whether such *a priori* selection of the responsible process precludes the contributions of other processes and whether such exclusion makes any difference in the predicted trends in island diffusion. The deeper question is, of course, whether it is possible to allow adatom islands to evolve as a function of time with mechanisms of their own choosing and thereby provide an unbiased illustration of the rate limiting step in the diffusion and the relative contributions of various mechanisms. We have recently developed a self-learning approach to kinetic Monte Carlo (KMC) simulations (SLKMC) in which the combination of an automatic generation of a database of single and multiple atom (2 or more atoms) processes during the evolution of the system, and a pattern recognition scheme provides a possible answer to the above question.[30] Application[26] of this method to the diffusion of 2D Cu islands on Cu(111) containing 19–100 atoms has shown the

diffusion coefficient D to scale with the number of atoms N in the island as $D \propto N^{-1.57}$. Periphery diffusion in which single atoms hopped from one fcc site to another was found to be the dominant mechanism. Several types of single and multiple atom processes were also revealed in the collected database. However, the frequency of occurrence of multiple atom processes was small even for the smaller islands (19–20 atoms) and their contribution to the diffusion process decreased further with increasing size and decreasing temperature. The situation may be different for islands with fewer atoms in which concerted island motion might dominate the diffusion process.[28] These processes necessarily involve occupation or transit through the hcp sites, although their exact nature is not known *a priori*. Our aim here is to apply SLKMC to examine the trends in the diffusion of small (2–10 atoms) Cu islands on Cu(111). Since in the original version of the code adatoms are assumed to occupy only fcc hollow sites, and in light of the possible importance of the hcp site from the discussion above, we have also carried out MD simulations for further insights into the mechanisms controlling island diffusion. Indeed, the MD simulations reveal the importance of processes involving concerted island motion. A second set of SLKMC simulations with an enhanced database is then performed and comparisons of the results of the two sets of KMC simulations provide an understanding of the factors that control the trends in the behavior, and the atomistic processes that determine the diffusive motion of small Cu islands on Cu(111). In particular, our results provide interesting insights into the conditions that may lead to anomalous diffusion coefficients for certain sizes of islands. Also, since the issue of the relative importance of the fcc and hcp site may be system specific, by carrying out these two sets of simulations, the results presented here should have significance for other surfaces.

II. CALCULATIONAL DETAILS

The first set of calculations are based on the recently developed self-learning kinetic Monte Carlo (SLKMC) (Ref. 30–32) technique, in which we have implemented a pattern recognition scheme that assigns a unique label to the environment of the diffusing atom up to several neighbors, for efficient storage and retrieval of information on activation energy barriers of possible processes that the system may choose to undergo. Provisions are made for automatic calculation of the energy barrier when a process is first identified and the result is stored in a database. These energy barriers are calculated using a simple method which maps out the total energy of the system as the diffusing entity moves from the initial fcc site to the aimed final fcc site, in small steps. During the ensuing energy minimization procedure, all atoms in the system are allowed to relax in all directions, except for the diffusing atom whose motion is constrained along the reaction path. Processes involving multiple atoms can thus be revealed naturally. Extensive comparisons of the resulting energy barriers[30] with those obtained using the more sophisticated nudged elastic band method show only minor differences. The simpler method gives a gain of almost two orders of magnitude in the time taken to acquire a comprehensive

database. To ensure that the principle of detailed balance is rigorously obeyed, the barriers of the forward processes are used, together with the total energies of the system in the initial and final states, to determine the energy barriers for the reverse processes. For the calculation of the total energy of the system, interatomic potentials based on the embedded atom method (EAM) are used. The initial step in the simulation is the acquisition of the database. Once it has become stable, i.e., no new processes appear for some time (for the islands under consideration the database saturated after about ten million KMC steps), the system evolves smoothly through atomistic processes of its choice and statistics are collected for calculating quantities like the mean square displacement of the center of mass of the island, correlation functions, and the frequencies of the atomistic processes.

In the SLKMC code which is extensively used here, we allow island atoms to occupy only fcc hollow sites. Also, interlayer exchange processes are not considered as the pattern recognition scheme for them is more complex than the one implemented here for diffusion via atomic hops. For the diffusion of 2D islands on Cu(111) such exchange processes are not expected to play a major role, as their energy barriers are relatively high. Furthermore, they have not been identified in either experiments or in the accompanying MD simulations performed at 500 K.

Assuming the validity of the transition state theory, the rate for an atom to hop to a vacant site is given by $r_i = \nu_i \exp(-\Delta E_i / k_B T)$. Here ΔE_i is the activation energy barrier, k_B is the Boltzmann constant, and ν_i is the attempt frequency or the so-called prefactor, which in principle can be sensitive to the details of the atomic environment. The prefactors for the various processes can thus be expected to be different. However, calculation of prefactors is nontrivial although the methodology is well defined.[22] Recent calculations of the prefactors for concerted island motion containing 2–7 atoms show some variation with size[28] particularly for the 7-atom island, and thus we have varied the prefactor for the 7-atom island by on order of magnitude and find the results reported here to remain essentially unchanged. In principle it would be preferable to calculate the prefactors for all the processes present in the database. We leave these calculations for the future, and invoke here the often used assumption of a standard value of 10^{12} s^{-1} for all prefactors. For further efficiency in the KMC algorithm, we have employed the Bortz-Kalos-Lebowitz (BKL) updating scheme[33] which allows one to reach macroscopic time scales of seconds or even hours for simulations at, say, room temperature as has been shown in recent works.[24,34]

For reasons discussed in the Introduction, MD simulations were also carried out to identify novel processes that cannot be automatically picked up in SLKMC runs because of its restrictions to fcc site occupancy. The MD simulations were carried out using standard techniques and, naturally, with the same EAM interatomic potentials as in the rest of the work. For efficiency, these simulations were performed at 500 K. As we shall see, collective island motion was revealed in the MD simulations and the hcp sites were found to be occupied particularly in transiting from one set of fcc sites to another. The message from the MD simulations is clear; the occupancy of the hcp site has to be allowed in KMC simulations

of small islands. The first step in the direction is to replace the original 3-shell pattern recognition scheme in SLKMC with a 9-shell one which provides labels to all fcc and hcp sites in the vicinity of the moving atoms. The labels of all processes collected in the SLKMC database can then be converted to the 9-shell scheme. For the 2-4 atom islands this was not a problem and all processes in the database were relabeled and new ones from MD simulations accordingly labeled and their energy barriers calculated and stored. This newer version of the code named SLKMC2 is fully equipped for the examination of the diffusion of these small Cu clusters on Cu(111). For islands containing 5 or more atoms, however, the database collected by SLKMC was far too extensive to manually convert each one into the new 9-shell labeling scheme. We have thus refrained from developing manually a database of all single and multiple atom and collective island diffusion processes for these larger Cu islands. Work is underway to equip SLKMC2 with an efficient and robust saddle point search routine such that in the future it will be able to acquire automatically the database of all relevant diffusion processes for two-dimensional islands of any size. For purposes here we have used SLKMC2 to examine the diffusion 2–4 atom Cu islands on Cu (111) in the presence of all possible single and multiple atoms, and collective island diffusion processes. The results of such simulations are compared with those obtained from SLKMC. Note that although concerted island motion is a type of multiple atom process, throughout this paper we have made a distinction between it and other multiple atom processes.

In the case of clusters with 5–10 atoms, we have proceeded along another route. We have retained the original SLKMC code and supplemented its database with processes that allow us to mimic collective island motion through an indirect procedure for the inclusion of the fcc-hcp jumps. The rationale for the indirect procedure is as follows. We know that the first step in a concerted island motion is the collective jump of all island atoms from fcc to hcp sites. For the island sizes in questions we calculate the activation energy barriers ΔE_{hf} for all such collective processes (fcc-hcp). MD simulations have been very helpful in revealing the shapes of the islands before the jumps from fcc to hcp sites. In particular, islands are found to assume more or less compact shapes before the collective jumps. The rate of the concerted island motion from fcc to hcp sites is $\nu_{hf} \times \exp(-\Delta E_{hf} / k_B T)$, where ν_{hf} is the pre-exponential factor, as noted above. As will be seen in Figs. 7 and 9, once the island atoms are in hcp sites, each one can hop to one of three equivalent fcc sites. We calculate the energy barriers for such collective hcp to fcc transitions. The relative magnitude of these barriers determines the relative probability for the particular hcp-fcc hop. If the energy barrier for all three processes is the same, then the probability for each is 1/3. In such a scenario the rate for fcc-hcp-fcc concerted island motion could be written as $1/3 \nu_{hf} \exp(-\Delta E_{hf} / k_B T)$ and in general as $P_{hf} \nu_{hf} \exp(-\Delta E_{hf} / k_B T)$, where P_{hf} is the probability of the particular hcp to fcc hop, which lies between 1 and 1/3. We now have a recipe for including concerted island motion from fcc to fcc sites in the database of SLKMC. To check whether the indirect procedure of including concerted island motion in SLKMC is reliable, we have

TABLE I. Diffusion coefficients of a trimer and a tetramer at different temperatures.

Island	Temperature (K)	SLKMC	(SLKMC+concerted motion) Indirect results	[SLKMC2+concerted motion] Direct results
Trimer	300	1.37×10^6	(2.78×10^{10})	$[4.89 \times 10^{10}]$
	500	5.26×10^8	(1.83×10^{11})	$[3.27 \times 10^{11}]$
	700	6.17×10^9	(4.55×10^{11})	$[1.22 \times 10^{12}]$
Tetramer	300	1.21×10^4	(3.40×10^9)	$[4.19 \times 10^9]$
	500	2.66×10^7	(9.17×10^{10})	$[1.06 \times 10^{11}]$
	700	6.35×10^8	(3.38×10^{11})	$[4.60 \times 10^{11}]$

carried out simulations for the 2–4 atoms islands using this recipe and compared the results obtained from SLKMC2. In Table I we have summarized the results of KMC simulations for trimers and tetramers by using the direct and indirect methods. As can be seen both yield almost the same diffusion coefficients.

As for the model system, we consider a fcc(111) substrate with an adatom island on top, as shown in Fig. 1. The gray circles are substrate atoms which stay rigid during the simulation, whereas the dark (colored on-line) circles are the island atoms, placed on fcc sites which are the hollow sites having no atoms underneath them in the layer below. A KMC simulation step begins by placing an adatom island of desired size, in a randomly chosen configuration, on the substrate. The system evolves by performing a process of its choice, from the multitude of possible single or multiple adatom jumps at each KMC step. We performed about 10^7 such

steps at 300 K, 500 K, and 700 K. Typically, at 500 K, 10^7 KMC steps were equal to 10^{-3} s in physical time. The diffusion coefficient of an adatom island is calculated by $D = \lim_{t \to \infty} \langle [R_{CM}(t) - R_{CM}(0)]^2 \rangle / 2dt$, where D is the diffusion coefficient, $R_{CM}(t)$ is the position of the center of mass of the island at time t, and d is the dimensionality of the system.

III. RESULTS AND DISCUSSIONS

We present first the results that are obtained from the SLKMC method with single and multiple atom processes involving jumps from one fcc site to another, which are automatically accumulated and performed during the simulation. The calculated diffusion coefficients of the islands at 300 K, 500 K, and 700 K are summarized in Table II. These are the numerical values in the first entry for each size type in Table II and range from 8.82×10^{10} Å^2/s for the dimer to

TABLE II. Diffusion coefficients of 1–10 atom islands at different temperatures and their effective diffusion barriers with diffusion prefactors.

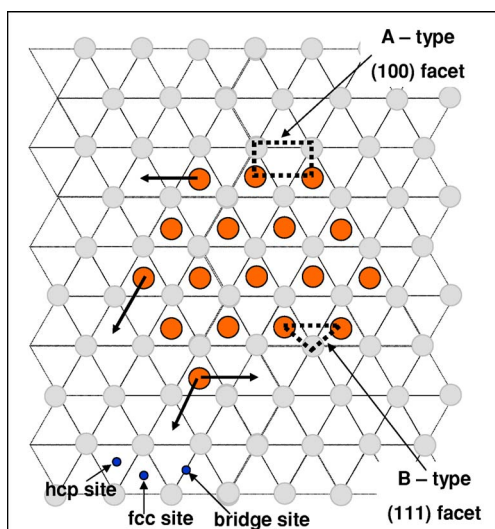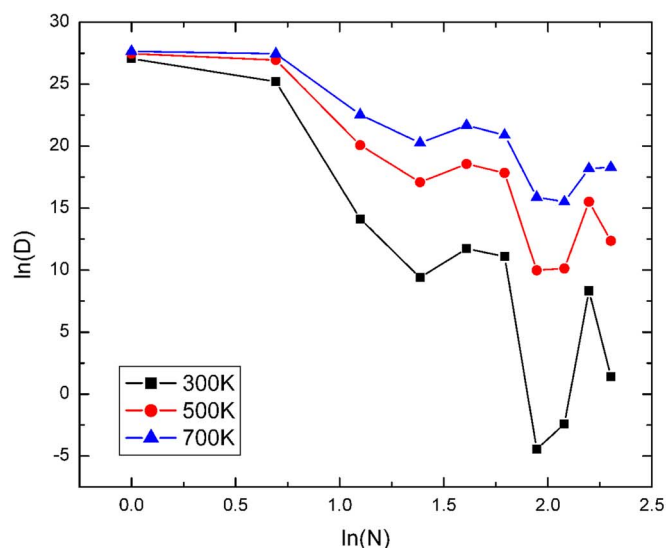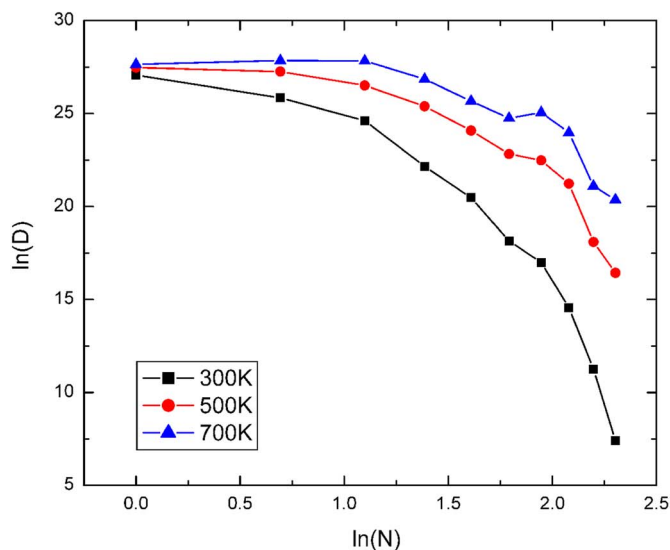| Island size (atoms)	Diffusion coefficient $D(\text{Å}^2/\text{s})$ KMC [KMC+concerted motion] 300 K	500 K	700 K	Effective barrier E_a (eV)	Diffusion prefactor $D_0(\text{Å}^2/\text{s})$
1	5.70×10^{11}	8.50×10^{11}	1.02×10^{12}	0.026	1.56×10^{12}
2	8.82×10^{10}	5.07×10^{11}	8.50×10^{11}	0.104	5.14×10^{12}
	$[1.68 \times 10^{11}]$	$[6.90 \times 10^{11}]$	$[1.24 \times 10^{12}]$	[0.091]	$[5.58 \times 10^{12}]$
3	1.37×10^6	5.26×10^8	6.17×10^9	0.380	3.52×10^{12}
	$[4.89 \times 10^{10}]$	$[3.27 \times 10^{11}]$	$[1.22 \times 10^{12}]$	[0.141]	$[1.06 \times 10^{13}]$
4	1.21×10^4	2.66×10^7	6.35×10^8	0.492	2.31×10^{12}
	$[4.19 \times 10^9]$	$[1.06 \times 10^{11}]$	$[4.60 \times 10^{11}]$	[0.211]	$[1.50 \times 10^{13}]$
5	1.25×10^5	1.16×10^8	2.60×10^9	0.440	4.13×10^{12}
	$[7.81 \times 10^8]$	$[2.87 \times 10^{10}]$	$[1.40 \times 10^{11}]$	[0.234]	$[6.73 \times 10^{12}]$
6	6.66×10^4	5.58×10^7	1.19×10^9	0.440	1.69×10^{12}
	$[7.57 \times 10^7]$	$[8.15 \times 10^9]$	$[5.60 \times 10^{10}]$	[0.300]	$[8.22 \times 10^{12}]$
7	1.18×10^{-2}	2.18×10^4	8.00×10^6	0.922	3.80×10^{13}
	$[2.40 \times 10^7]$	$[5.80 \times 10^9]$	$[7.60 \times 10^{10}]$	[0.362]	$[2.90 \times 10^{13}]$
8	9.00×10^{-2}	2.53×10^4	5.49×10^6	0.800	3.70×10^{12}
	$[2.10 \times 10^6]$	$[1.65 \times 10^9]$	$[2.59 \times 10^{10}]$	[0.430]	$[3.61 \times 10^{13}]$
9	4.18×10^3	5.50×10^6	8.00×10^7	0.448	1.55×10^{11}
	$[7.72 \times 10^4]$	$[7.20 \times 10^7]$	$[1.45 \times 10^9]$	[0.444]	$[2.24 \times 10^{12}]$
10	4.12	2.33×10^5	8.82×10^7	0.731	7.24×10^{12}
	$[1.65 \times 10^3]$	$[1.37 \times 10^7]$	$[7.02 \times 10^8]$	[0.580]	$[1.06 \times 10^{13}]$

FIG. 1. (Color online) Some examples of adatom diffusion and hops on the fcc(111) surface. Dark-colored atoms are active and placed at fcc sites, whereas light-colored atoms serve as the substrate. The lower edge of the layer containing active atoms forms a (111) microfacet, so it is called the B-type step edge while the upper edge of the layer containing active atoms forms a (100) microfacet which is called an A-type step.

4.12 $Å^2$/s for the 10-atom island. A log-log plot of D vs N in Fig. 2(a) shows oscillations in the diffusion coefficient with size. This hint for magic sizes of islands signifying reduced mobility is also seen in the Arrhenius plot of $\ln D$ vs $1/k_B T$. The effective diffusion barriers extracted for each island size from the Arrhenius plot (Fig. 3) also display oscillatory behavior. As can be seen in Table II, the 3, 7, and 10-atom islands display higher effective barriers than the others. The barrier for diffusion is particularly high for the perfect hexagon (7-atom) island.

As we mentioned in Sec. II, MD simulations carried out at 500 K revealed several new concerted moves of the islands which involved occupation of the hcp sites, too. Before discussing the details of the atomistic processes let us examine the results for the diffusion coefficients once these processes are included in the database of SLKMC. The calculated diffusion coefficients, effective energy barriers, and the prefactors for the second set of KMC simulations are summarized in Table II. These values are given in the square brackets underneath the corresponding ones obtained when hcp-site assisted processes are not included. The size dependence of the diffusion coefficients at three different temperatures with the inclusion of concerted moves from MD are also shown in Fig. 2(b) for comparison of the case already discussed in Fig. 2(a). Further comparison of the results of the two sets of simulations is in Fig. 3, in which the effective diffusion energy barrier appears to scale with the island size once the hcp-assisted concerted motion is taken into account. The striking result is that there is no longer any oscillation in the quantities and the 3 and 7 atom islands diffuse just like the others, in proportion to their size. We now turn to an analysis of the details of the single and multiple atom mechanisms involved in the diffusion of the islands, one by one.

(a)

(b)

FIG. 2. (Color online) Diffusion coefficients as a function of the island size; (a) KMC results without including concerted motion mechanisms; (b) KMC results after including concerted motion mechanisms obtained from MD simulations.

A. Monomer

For completeness we begin with a few comments on the diffusion of an adatom on Cu(111). The primary motion for a single atom is simply the process of hopping between the fcc and the hcp sites. We find an activation energy barrier of E = 29 meV for the process, while with a slightly different EAM potential Marinica *et al.*[28] find it to be 41 meV. As already mentioned, exchange processes between the adatom and the substrate atoms are not included in our KMC simulations, neither do they appear in the accompanying MD simulations. The effective diffusion barrier inferred from the Arrhenius plot of the monomer diffusivities from our KMC simulations is E_a=26±3 meV, which is consistent with the
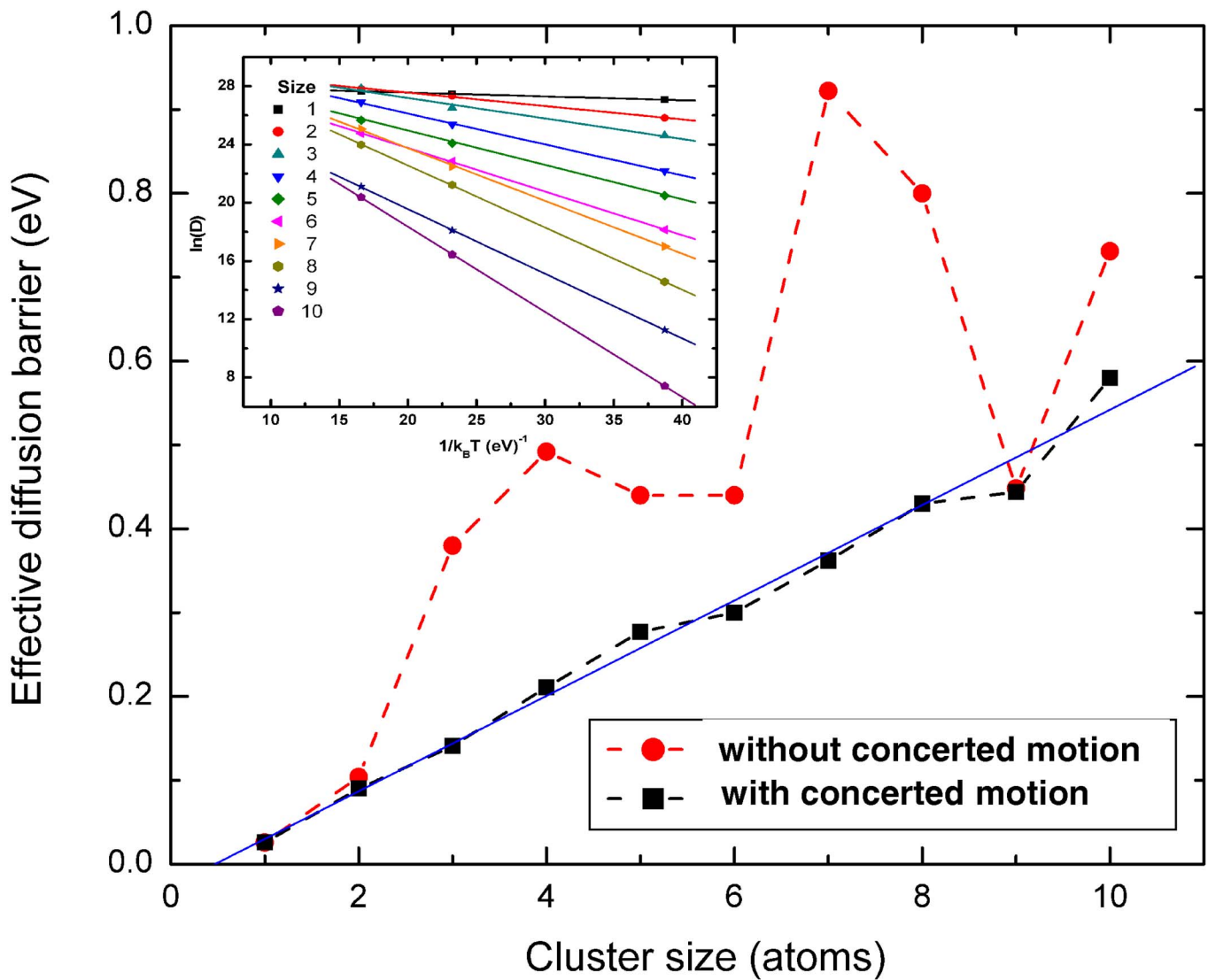
FIG. 3. (Color online) Effective diffusion barriers of 1–10 atom islands plotted as a function of island size. The dotted line with squares represents full KMC simulation results including concerted motion, whereas the dotted line with circles shows results of the KMC simulation without including concerted motion mechanisms. The inset shows Arrhenius plots of diffusion coefficients as a function of temperature.

calculated energy barrier contained in our database. This value is also in agreement with that obtained from MD simulations (E_a=31.0±0.8 meV) by Hynninen *et al.*[23] Experimental results report the adatom activation energy on Cu(111) to be E_a=37.00±5 meV.[9] Our results are thus in agreement with experimental data.

B. Dimer

In the case of the motion of the dimer the SLKMC code picked up only two mechanisms which permit jumps from fcc to fcc sites. These are labeled dimer A and dimer B in Fig. 4(a), and their energy barriers are 101 meV and 15 meV, respectively. Results of diffusion coefficients with these two processes at three different temperatures are in Table II. The effective diffusion barrier for the dimer from the Arrhenius plot is 104 meV. Of course, the dimer motion is actually nontrivial since in reality both dimer atoms could

also occupy the hcp sites or mixed sites with one atom on the fcc and the other on the hcp site. The MD simulations actually revealed 13 more mechanisms for the dimer diffusion which are shown in Fig. 4(b). These illustrations show transitions between the sites occupied by the dimer atoms. Simultaneous occupation of mixed sites is slightly favorable because of the somewhat lower energy (by 1–3 meV), as compared to both atoms occupying the same type of sites.

Let us have a critical look at mechanisms shown in Fig. 4(b). Processes describing sliding and rotational motion, D_2, D_3, D_4, D_6, and D_8, have lower energy barriers as compared to the others shown in Fig. 4(b). Process D_2 in which both atoms are initially on hcp sites and one jumps to the fcc site by crossing the bridge site, has the lowest energy barrier of 5 meV, The second low energy mechanism is D_6 (9 meV), in which both atoms occupy fcc sites initially and one of them jumps to hcp site by crossing the bridge site. The energy barrier for the same mechanism from the experimental
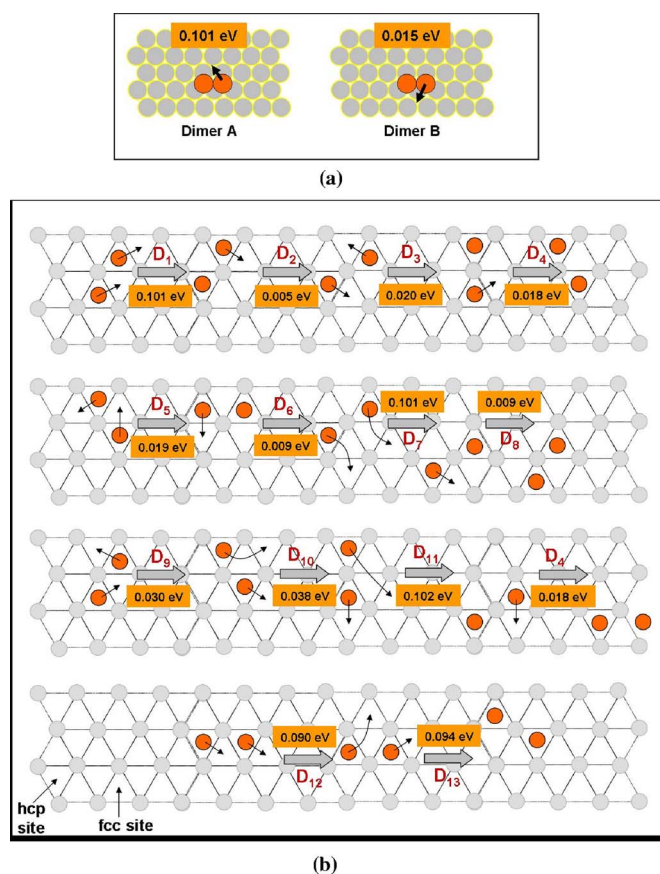
(a)

(b)

FIG. 4. (Color online) (a) Illustration of two simple mechanisms for dimer diffusion and their energy barriers, where atoms jump from fcc to fcc sites. (b) 13 mechanisms for dimer diffusion via fcc to hcp sites and their energy barriers. These mechanisms were found from MD simulations.

data reported by Repp *et al.*[9] is 18 ± 3 meV, which is larger than what we find. Marinica *et al.*[28] find this barrier to be 16 meV. Process D_4 describes dimer atoms as initially occupying mixed sites and finally both atoms occupying hcp sites. We find its energy barrier to be 18 meV while Marinica *et al.*[28] reported it to be $E=26$ meV. We also observed long jump mechanisms (D_7, D_{10}, D_{11}, and D_{13}) for dimer diffusion in our MD simulations.

The sliding motion between fcc and hcp sites has diffusion barriers of the same order of magnitude as that for the long jump motion of the dimer. On the other hand, the rotational motion, D_3, has a diffusion barrier (20 meV) closer to the value of a single atom hopping barrier, which is 29 meV. Finally, we included all of these 13 mechanisms in our SLKMC database that had only two mechanisms (dimer A and dimer B) initially. As we can see from Table II, with the inclusion of concerted motion the effective diffusion barrier reduces to $E_a=92$ meV, which is closer to the value of barrier representing concerted motion of the dimer. Although a dimer performs low energy mechanisms (D_2, D_3, D_4, D_6, and D_8) more frequently, the change in the center of mass position is small as compared to the long jump mechanisms (D_7, D_{10}, D_{11}, and D_{13}) and also concerted motion mechanism (D_1 and D_{12}). Hence a small frequency of relatively high energy mechanisms (long jumps) can greatly change the cen-

ter of mass position of the dimer. This is why the effective diffusion barrier of dimer is closer to the diffusion barrier of long jumps and concerted motion mechanisms (D_7, D_{11}, D_{13}).

C. Trimer

We have done a detailed study of trimer diffusion using SLKMC simulations. There are only nine possible atom-by-atom motion mechanisms which were identified by our SLKMC code. These mechanisms and their corresponding energy barriers are shown in Fig. 5(a). With only fcc to fcc jumps the effective diffusion barrier for the trimer is 380 meV (see Table II). Actually the atom-by-atom motion produces a shape change but does not facilitate the diffusion of the trimer. We obtained quite interesting results when we included mechanisms describing concerted motion of trimer as shown in Fig. 5(b). Trimer moves from one fcc site to the neighboring hcp site by performing concerted gliding and rotation mechanisms. The energy barrier for concerted gliding of the trimer from 3 fB to 3 hA is found to be 125 meV, whereas the reverse mechanism has a barrier of 115 meV. The rotation of the trimer has the lowest energy barrier of all: 38 meV from 3 hA to 3 fA and 62 meV from 3 fA to 3 hA, respectively. With the inclusion of these additional processes the effective diffusion barrier is found to be 141 meV.

This is a dramatic reduction from 380 meV found earlier and the effect is impressively represented in Figs. 2(b) and 3(b) which shows the trimer to be relatively mobile. In Fig. 6 we plot the distribution of the frequency of events with and without rotation and concerted motion, represented, respectively, by filled and open symbols. We find that the occurrence frequencies of added mechanisms (concerted motion and rotation) are much higher than the occurrence frequencies of all other nine mechanisms because concerted motion and rotation mechanisms have low energy barriers as compared to the mechanisms such as *opening from A* and *opening from B*. Although rotation dominates, it does not play a key role in trimer diffusion because it is not responsible for the center of mass motion of the trimer. We expect concerted motion to dominate diffusion, and thus we can predict that the value of the effective diffusion barrier should be closer to the value of the concerted motion barrier, which is indeed true here. In Table II, we can clearly see the difference between results before and after including rotation and concerted motion mechanisms in our primary database of nine processes.

D. Tetramer

In the case of the tetramer we have 28 possible, fcc to fcc, atom-by-atom jump processes which together with their energy barriers are shown in Fig. 7(a). As noted in Table II, KMC simulations performed with these mechanisms led to an effective diffusion barrier of 492 meV. Three mechanisms exhibiting concerted motion and shearing of a diamond shaped tetramer, revealed in MD simulations, and their corresponding diffusion barriers, are shown in Fig. 7(b). Concerted motion of a diamond shaped tetramer takes place through sliding between the fcc and the hcp sites, along its small and large diagonals. The ones along the small diagonal
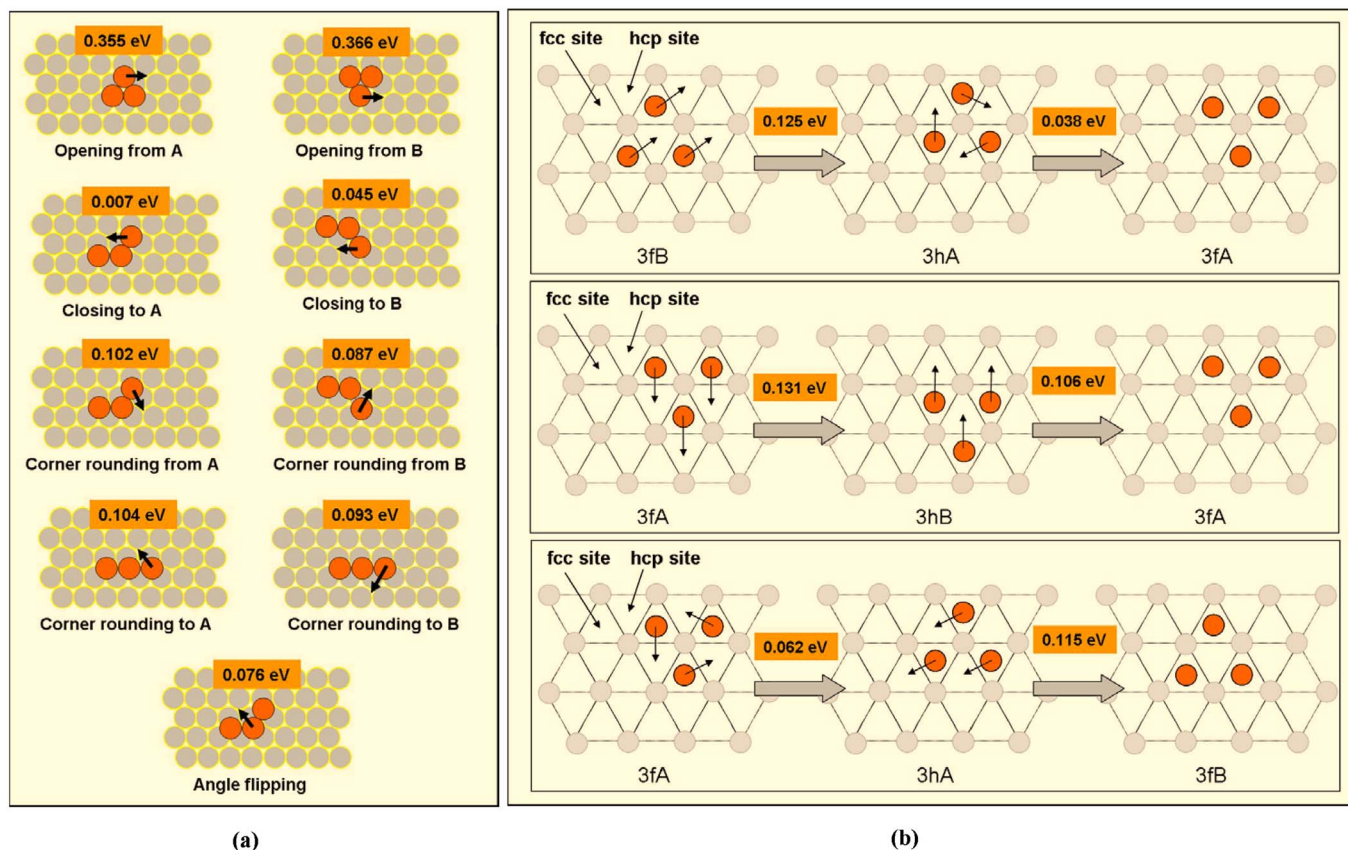
FIG. 5. (Color online) (a) Nine mechanisms for trimer diffusion with their corresponding energy barriers, where atoms are allowed to jump from fcc to fcc sites. (b) Trimer diffusion mechanisms observed during MD simulations. These mechanisms are conducted through a collective motion of three atoms by rotation and gliding over the bridge sites from fcc to hcp sites, or vice versa.

[Fig. 7(b)1] have lower energy barrier (167 meV for fcc to hcp and 125 meV for hcp to fcc) than those along the large diagonal [Fig. 7(b)2]. These processes have also been discussed by Marinica *et al.*[28] However, the case of diamond shaped tetramer diffusion through shearing mechanism shown in Fig. 7(b)3 with energy barrier 230 meV was not taken into account by them. When we included these three mechanisms in our database of 28 single atom mechanisms and performed KMC simulation, we found significantly different values for the diffusion coefficients. In Table II, these values are written in square brackets and the effective diffusion barrier for tetramer is $E_a = 212$ meV.

E. Islands containing 5–10 atoms

A few examples of single atom processes collected in the database of our KMC simulations, for the islands containing 5–10 atoms, are shown in Fig. 8 with the corresponding energy barriers. The diffusion coefficients calculated from KMC simulations based on these single atom mechanisms are very low, as shown in Table II. This is particularly the case for the 7 and 8 atom islands whose effective diffusion barriers are consequently the largest. This is understandable because we find that processes such as *AB corner detachment A* and *AB corner detachment B*, shown in Fig. 8, play a key role in the island diffusion by contributing the most to the change in the center of mass position. Processes such as
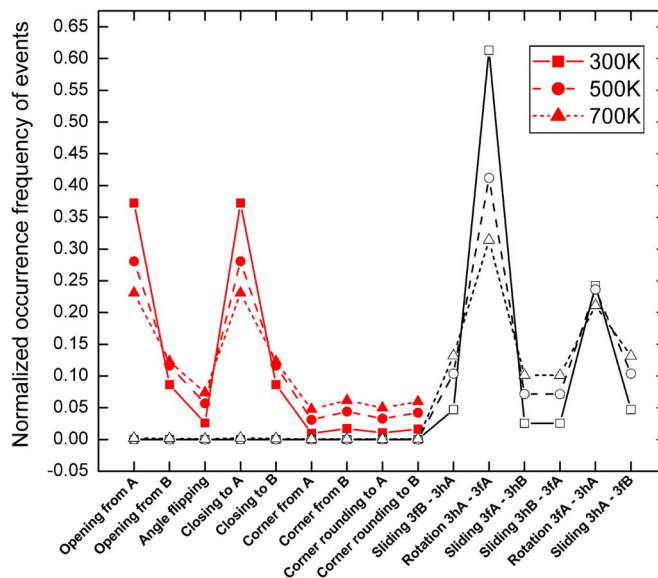

FIG. 6. (Color online) Distribution of normalized frequencies of event occurrences in the case of trimer diffusion. The lines with filled symbols show the distributions of events at different temperatures when only single atom mechanisms were included, and lines with open symbols show the distributions of all events including the collective motion of three atoms by rotation and gliding.
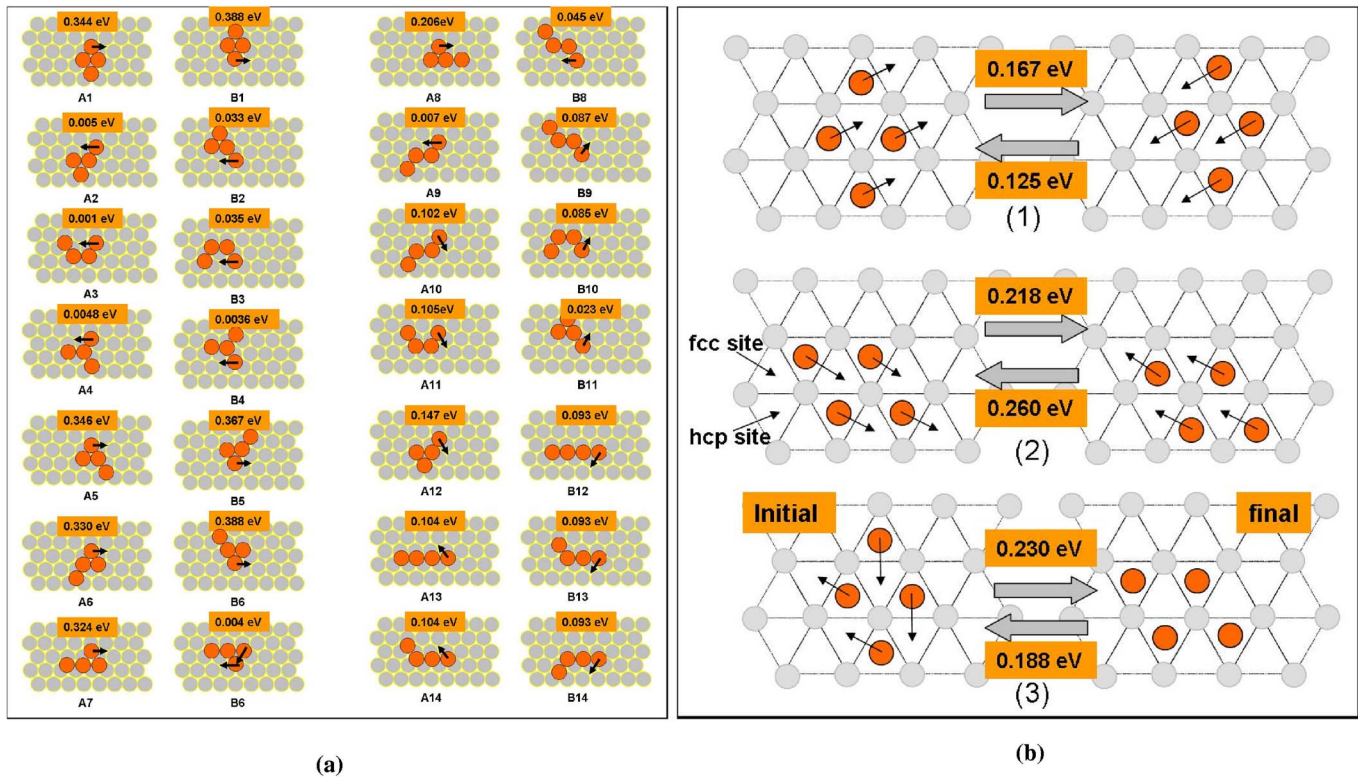
(a)   (b)

FIG. 7. (Color online) (a) Illustration of 28 mechanisms and their corresponding energy barriers for tetramer diffusion, where jumps are allowed from fcc to fcc sites only. (b) Tetramer diffusion mechanisms revealed from MD simulations: (1) diagonal glide, (2) vertical glide of 4-atom island over the bridge sites and the corresponding energy barriers, and (3) shearing mechanism.

step edge A and *step edge B* occur more frequently, but they do not contribute significantly to the motion of the center of mass of the island; rather the atoms move around and around along the periphery of the island. In Fig. 9 we show the concerted motion processes revealed from MD simulations. Their energy barriers were determined from molecular static calculations by dragging the central atom of the island from fcc to the nearest hcp site. Other atoms in the island followed its motion by gliding over the bridge sites. The different shapes and geometries of these islands contribute to the differences in the energy barriers for the processes. For example in our MD simulations we found that the 10-atom island can move as a single entity from fcc to hcp sites whenever it appears into one of the three shapes shown in Fig. 9. The energy barriers associated with these processes are slightly different. Clearly, the barriers of these concerted motion mechanisms (for 5–10 atom islands) are comparatively lower (270–590 meV) than the energy barriers of the single atom mechanisms *AB corner detachment A* and *AB corner detachment B*, also considered essential for island diffusion. After the inclusion of new low energy concerted motion mechanisms in our database, the high energy single atom mechanisms become less frequent in KMC simulations and high values of diffusion coefficients and correspondingly low values of the effective diffusion barriers were obtained (see Table II). The size-dependent oscillations of the diffusion coefficients and the effective diffusion barriers also disappeared from the plots shown in Fig. 2(b) and Fig. 3, respectively. We can thus conclude that the absence of the low
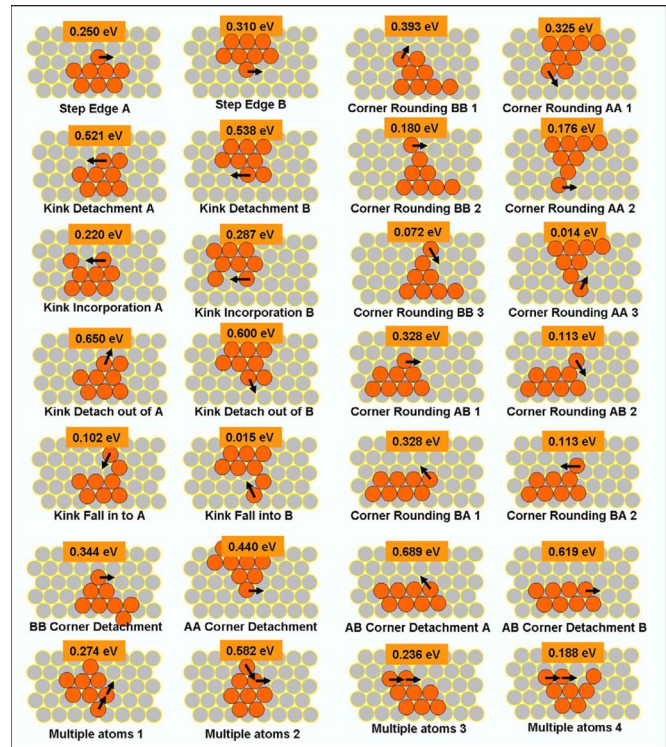

FIG. 8. (Color online) A few examples of single and multiple atom mechanisms and their corresponding energy barriers used in our KMC simulations for islands larger than 4 atoms. Jumps are allowed from fcc to fcc sites only.
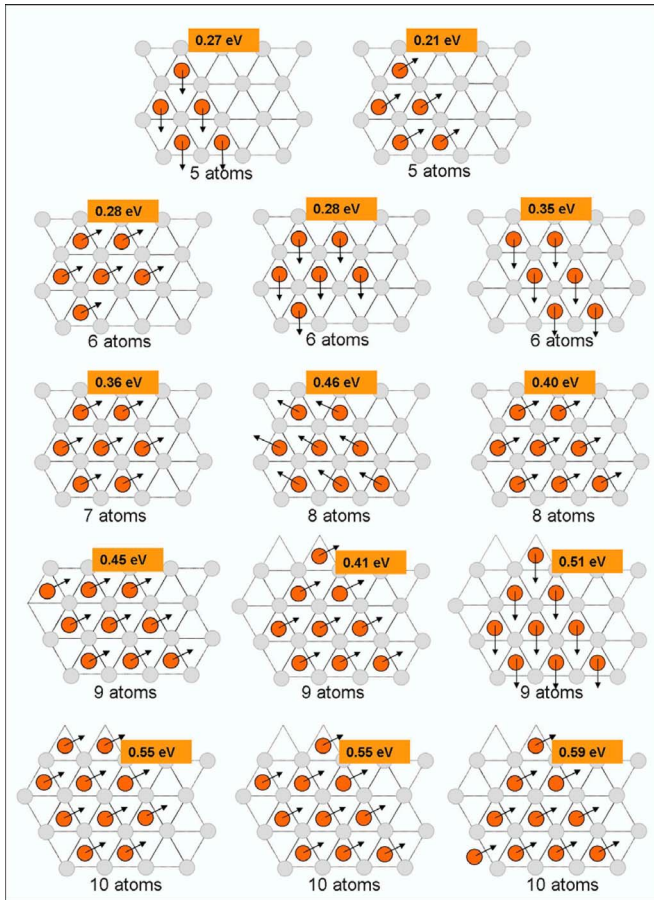
FIG. 9. (Color online) Diffusion mechanisms found by performing MD simulations for the island sizes of 5–10 atoms and their corresponding energy barriers when they glide over the bridge sites exhibiting collective motion of all atoms.

energy concerted motion mechanisms is responsible for the oscillatory behavior of diffusion coefficients as the function of size. Finally, our complete KMC results show that the effective diffusion barriers increase almost monotonically with increasing island size.

F. Key mechanisms and their occurrence frequencies

In Fig. 10 we show the normalized frequencies of all events from the extended SLKMC data that were performed during the simulations. Lines with open symbols in Fig. 10 show the occurrence frequencies of the all concerted motion mechanisms, at three different temperatures, as the function of the island size, while those with filled symbols all single atom mechanisms. For the dimer case, most of the single atom mechanisms have the same effective barriers as compared to the barriers associated with concerted motion mechanisms. Thus, the occurrence frequencies of single and multiple atom mechanisms are almost the same for dimer diffusion. In the case of 3–7 atom islands, concerted motion processes are associated with significantly lower energy barriers as compared to the single atoms, and therefore concerted motion occurs more frequently. A 6-atom island has an effective barrier for concerted motion that is closer to barri-
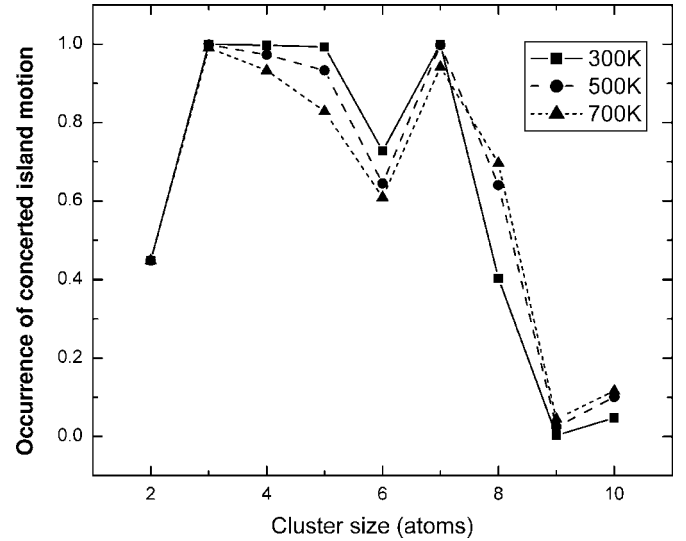

FIG. 10. Distribiution of normalized frequencies of concerted motion events as a function of the island size.

ers of some single atom mechanisms, which play a role in the motion of the center of mass position to some extent (i.e., *step edge A* and *step edge B* processes). Because of the close competition between concerted motion and single atom mechanisms, we find a narrow gap between their occurrence frequencies in the case of a 6-atom island. A similar, narrow gap can be seen in the case of the 8-atom island. In this case there is close competition between concerted motion and the motion of the single atom going around the periphery of the island (i.e., *BB corner detachment* and *AA corner detachment* processes). In the case of 9 and 10 atom islands the low energy single atom mechanisms (i.e., *step edge A* and *step edge B* processes) occur more frequently, but they do not play a key role in island diffusion. On the other hand, since the barriers of the concerted motion mechanisms are higher (410–590 meV), they occur rarely but still play an important role in the diffusion.

IV. CONCLUSIONS

To summarize, we have performed a systematic study of the diffusion of small Cu islands on Cu(111), using a recently developed self learning KMC simulations in which the system is allowed to evolve through mechanisms of its choice with the usage of a self-generated database of single and multiple atom diffusion processes. Complementary molecular dynamics simulations carried out for a few cases provided further details of several new mechanisms for small island diffusion which were not automatically picked up by our SLKMC method because of the initial restriction of fcc site occupation. We found significant changes in the size-dependent variations of diffusion characteristics of the islands after including concerted motion mechanisms which were revealed from MD simulations. We find that these small-sized islands diffuse primarily through concerted motion with a small contribution from single atom processes, even though for certain cases the frequency of single atom processes is large because of lower activation energies. By

allowing the system the possibility of evolving in time through all types of processes of its choice, we are able to establish the relative significance of various types of atomistic processes through considerations of the kinetics and not just the energetics and/or the thermodynamics, as is often done. For small Cu islands on Cu(111), we find the effective barriers for diffusion to scale with island size. We await experiments to verify our findings.

[1] D. W. Bassett, J. Phys. C **9**, 2491 (1976).

[2] T. T. Tsong and R. Casanova, Phys. Rev. B **22**, 4632 (1980).

[3] S. C. Wang and G. Ehrlich, Surf. Sci. **239**, 301 (1990).

[4] S. C. Wang and G. Ehrlich, Phys. Rev. Lett. **68**, 1160 (1992).

[5] S. C. Wang, U. Kurpick, and G. Ehrlich, Phys. Rev. Lett. **81**, 4923 (1998).

[6] G. L. Kellogg, Appl. Surf. Sci. **67**, 134 (1993).

[7] J. M. Wen, S. L. Chang, J. W. Burnett, J. W. Evans, and P. A. Thiel, Phys. Rev. Lett. **73**, 2591 (1994).

[8] K. Morgenstern, G. Rosenfeld, B. Poelsema, and G. Comsa, Phys. Rev. Lett. **74**, 2058 (1995).

[9] J. Repp, G. Meyer, K. H. Rieder, and P. Hyldgaard, Phys. Rev. Lett. **91**, 206102 (2003).

[10] W. W. Pai, A. K. Swan, Z. Zhang, and J. F. Wendelken, Phys. Rev. Lett. **79**, 3210 (1997).

[11] M. Giesen, G. SchulzeIcking-Konert, and H. Ibach, Phys. Rev. Lett. **80**, 552 (1998).

[12] J. Ferrn, L. Gmez, J. M. Gallego, J. Camarero, J. E. Prieto, V. Cros, A. L. Vzquez de Parga, J. J. de Miguel, and R. Miranda, Surf. Sci. **459**, 135 (2000).

[13] H. A. van der Vegt, J. Alvarez, X. Torrelles, S. Ferrer, and E. Vlieg, Phys. Rev. B **52**, 17443 (1995).

[14] M. Giesen and H. Ibach, Surf. Sci. **529**, 135 (2003).

[15] C. Busse, C. Polop, M. Muller, K. Albe, U. Linke, and T. Michely, Phys. Rev. Lett. **91**, 056103 (2003).

[16] M. Muller, K. Albe, C. Busse, A. Thoma, and T. Michely, Phys. Rev. B **71**, 075407 (2005).

[17] C. L. Liu and J. B. Adams, Surf. Sci. **268**, 73 (1992).

[18] J. C. Hamilton, M. S. Daw, and S. M. Foiles, Phys. Rev. Lett. **74**, 2760 (1995).

[19] D. S. Sholl and R. T. Skodje, Phys. Rev. Lett. **75**, 3158 (1995).

[20] A. Bogicevic, S. Liu, J. Jacobsen, B. Lundqvist, and H. Metiu, Phys. Rev. B **57**, R9459 (1998).

[21] C. M. Chang, C. M. Wei, and S. P. Chen, Phys. Rev. Lett. **85**, 1044 (2000).

[22] U. Kurpick, P. Kurpick, and T. S. Rahman, Surf. Sci. **383**, L713 (1997).

[23] A. Hynninen, A. Al-Rawi, T. Ala-Nissila, and T. S. Rahman (unpublished).

[24] J. Heinonen, I. Koponen, J. Merikoski, and T. Ala-Nissila, Phys. Rev. Lett. **82**, 2733 (1999).

[25] P. Salo, J. Hirvonen, I. T. Koponen, O. S. Trushin, J. Heinonen, and T. Ala-Nissila, Phys. Rev. B **64**, 161405(R) (2001).

[26] T. S. Rahman, A. Kara, O. Trushin, and A. Karim (unpublished).

[27] S. M. Foiles, M. I. Baskes, and M. S. Daw, Phys. Rev. B **33**, 7983 (1986).

[28] M. C. Marinica, C. Barreteau, M. C. Desjonqueres, and D. Spanjaard, Phys. Rev. B **70**, 075415 (2004).

[29] Y. Mishin, M. J. Mehl, D. A. Papaconstantopoulos, A. F. Voter, and J. D. Kress, Phys. Rev. B **63**, 224106 (2001).

[30] O. Trushin, A. Karim, A. Kara, and T. S. Rahman, Phys. Rev. B **72**, 115401 (2005).

[31] We have now developed a SLKMC code which inherently uses the 9-shell pattern recognition scheme.

[32] T. S. Rahman, C. Ghosh, O. Trushin, A. Kara, and A. Karim, in *Nanomodeling*, Proceedings of SPIE, edited by Akhlesh Lakhtakia and Sergey A. Maksimenko (SPIE, Bellingham, WA, 2004), Vol. 5509.

[33] A. B. Bortz, M. H. Kalos, and J. L. Lebowitz, J. Comput. Phys. **17**, 10 (1975).

[34] M. Rusanen, I. T. Koponen, J. Heinonen, and T. Ala-Nissila, Phys. Rev. Lett. **86**, 5317 (2001).